



Exponential vaporization fronts and critical heat flux in pool boiling

C. Staszal, A.L. Yarin*

Department of Mechanical and Industrial Engineering, University of Illinois at Chicago, 842 W. Taylor St., Chicago, IL 60607-7022, USA



ARTICLE INFO

Keywords:

Heat transfer
Boiling crisis
Critical heat flux
Incipient boiling
Vaporization front

ABSTRACT

Here we study the inception and propagation of vaporization fronts and transition to the critical heat flux (CHF) and film-boiling regime triggered by a steep, almost instantaneous increase in the heat release from a strip heater submerged in Novec 7300 liquid. The propagation path of the resulting vaporization front along the strip heater is measured and shown to be exponentially increasing in time, in distinction from the previous reports in literature claiming that the increase is only linear. Since the previous experiments employed such liquids as water, refrigerants, acetone, ethanol, and alkali metals, which possess relatively high latent heat of evaporation and thus require a relatively high power to be supplied, the heater burnout at the inception of the CHF and film boiling was too fast to allow for longer-time observations. Accordingly, the previous works observed only an extremely short-time asymptotics of the propagation process, which means the short-time expansion of the exponential function, which is linear. On the other hand, in the experiments with Novec 7300 liquid, the heater burnout is delayed due to a much lower latent heat of evaporation, thus allowing for a much longer observation of the propagation path, which appears to be exponentially increasing in time. The experiments were preceded by our theoretical prediction of such a behavior, and this theory is also described in the present work. Due to the fact that this theory has been corroborated by the experimental data, the theory yields an adequate explanation and description of the CHF trigger and film boiling inception.

1. Introduction

Pool boiling, and especially the inception of the detrimental critical heat flux (CHF) regime, is a complicated physical phenomenon which is not fully understood, even though multiple experiments were conducted and revealed abundant empirical information [1,2]. Pool boiling is highly effective in heat removal since it involves significant latent heat of evaporation associated with the nucleate boiling regimes, which guarantees high heat fluxes. This is an attractive feature for cooling of high-power microelectronics in ground and space applications [3–7], metallurgical quenching [1], etc. The severe limitation on the heat removal in pool boiling, namely the inception of the boiling crisis or the CHF sets in in the most attractive domain of the heat flux regimes, which, unfortunately, results in a rapid, practically uncontrollable bubble merging at the heater surface and transition to film boiling. The resulting vapor film hovering over the heater surface drastically diminishes the heat removal rate, which leads to a rapid burnout of the heater and, in particular, to failure of microelectronics components. Different methods were employed to enhance heat removal in pool boiling, e.g. deposition of nanofibers on the heater surface [4–7], nanoporous textured finishes [8], embedded arrays of low-conductive epoxy

[9], modification of the surface wettability [10,11], and miniaturization [12]. Such measures were able to delay the CHF onset, but definitely not to fully eliminate it. Further works have also aimed at a better understanding of the boiling crisis and ascertained some aspects of the bubble merging as a critical percolation phenomenon [13], as well as attributed the heater dry-out at the onset of boiling crisis to the effect of the vapor recoil force at the bubble footprint [14]. Direct numerical simulation methods which aim at modeling of pool boiling, not to mention the CHF itself, are still insufficiently mature [5,15].

When a step-wise increase in power is experienced by a heating element, a direct transition to film boiling may occur, bypassing entirely the nucleate boiling regime, which is sometimes referred to as the third heat-transfer crisis [16–20]. Then, the nucleating bubbles on the heater surface rapidly spread, resulting in formation and propagation of vaporization fronts that merge and fully encase it. A number of works reported that vaporization fronts propagate with a constant velocity [18,19,21–24]. These works employed water (the latent heat of evaporation $L = 2260$ kJ/kg) [21,25], refrigerants ($L = 246.7$ kJ/kg for refrigerant FC-C318 Freon) [22,26], acetone ($L = 515$ kJ/kg) [16,27], ethanol ($L = 844$ kJ/kg) [20,27], alkali metals (for potassium $L = 2023$ kJ/kg, and for cesium $L = 497$ kJ/kg) [20,28], n-pentane

* Corresponding author.

E-mail address: ayarin@uic.edu (A.L. Yarin).

($L = 356$ kJ/kg), [23,29], etc. [17,24,30]. The assumption of a constant velocity of vaporization fronts was embedded as a cornerstone in a number of theories of the inception of this phenomenon [18,19,21,22]. It should be emphasized that all the liquids employed in such experiments so far, possess relatively high latent heats of evaporation, and accordingly, the heaters were subjected to a relatively high power supply to trigger vaporization fronts. As a result, the heaters were burnt very rapidly after the inception of the vaporization fronts, and in this short-time limit any dependence of the propagation path on time would be inevitably linearized resulting in pseudo-constant propagation velocities. Therefore, the real nature and character of the vaporization front incipience and propagation could be explored only in the experiments with liquids with the lowest latent heat of evaporation (e.g. Novec 7300 liquid with $L = 101.67$ kJ/kg), which allow for longer observation times. This is undertaken in the present work, with the corresponding theory of the transition to the CHF and film boiling proposed as well.

2. Experimental

2.1. Materials

For the experiments conducted here, 3M Novec 7300 liquid was used as a working fluid. The thermal diffusivity of Novec 7300 is $\alpha_L = 3.57 \times 10^{-8}$ m²/s, the density $\rho_L = (1.7162 - 0.0024 T) \times 10^3$ kg/m³ (with T being temperature in °C) [31]. The Kanthal A-1 flat resistive strips of 0.4 mm \times 0.1 mm (width \times thickness) and 0.5 mm \times 0.1 mm (width \times thickness), both 30 mm in length, were used as the heating elements.

2.2. Experimental setup

Experiments were conducted using the setup shown in Fig. 1. The pool filled with Novec 7300 liquid was made of two aluminum and two borosilicate glass walls. The two opposing borosilicate glass walls allowed for the observations using a high-speed camera. The other two walls and the bottom were made of aluminum. A polycarbonate plate with a through hole (to sustain the free surface of the liquid at the atmospheric pressure) was located on top to act as a condenser and to

minimize the loss of Novec 7300 liquid. An additional stainless steel resistive wire heater was inserted in the pool (cf. Fig. 1a) to heat up the working fluid close to the boiling temperature (the saturation temperature at the atmospheric pressure of Novec 7300 is 98 °C). The temperature of the liquid in the pool was monitored by a thermocouple (Omega 5TC-TT-T-30-30).

A specially designed fixture, Fig. 1c, was used to clamp the flat Kanthal resistive strip. After each experiment with the vaporization front inception, the resistive strip was replaced. The strip was horizontal and stretched between two copper plates mounted at the opposing sides of a polycarbonate fixture to ensure the electrical contact (cf. Fig. 1c). A threaded rod disjoined the lower part of the polycarbonate fixture to stretch the strip (the heating element) and to ensure that it would be straight and horizontal. The copper plates were connected to a DC power supply which was triggered to provide a practically instantaneous step-wise increase in the Joule heat flux in the Kanthal resistive strip.

The applied voltage at the strip was monitored using an oscilloscope (Tektronix model TDS 210) connected to the copper plates. A multimeter (Fluke model 8845A) was also used to measure the strip resistance prior to the experiments. It should be emphasized that the Kanthal strip used as the heating element possessed the coefficient of temperature $CT = 1.0$ in the temperature range of up to 480 °C. That means that the strip resistance practically did not change in spite of the Joule heating. Thus, the resistance measured at room temperature was used in the calculations of the heat flux q , as $q = V^2/AR$, where V is the voltage measured by the oscilloscope, A is the total surface area of the strip, and R is the resistance of the Kanthal strip measured by the multimeter at room temperature.

2.3. Observation

The inception and propagation of vaporization fronts on the strip heater resulting from a nucleated bubble was recorded by a high-speed camera (Phantom V210) at 10,000 fps using an LED light source for illumination. Snapshots were extracted from the video and analyzed using ImageJ to calculate the initial radius of the nucleated bubble and track the location of the vaporization front in time. Then, the velocity of the vaporization front was also calculated.

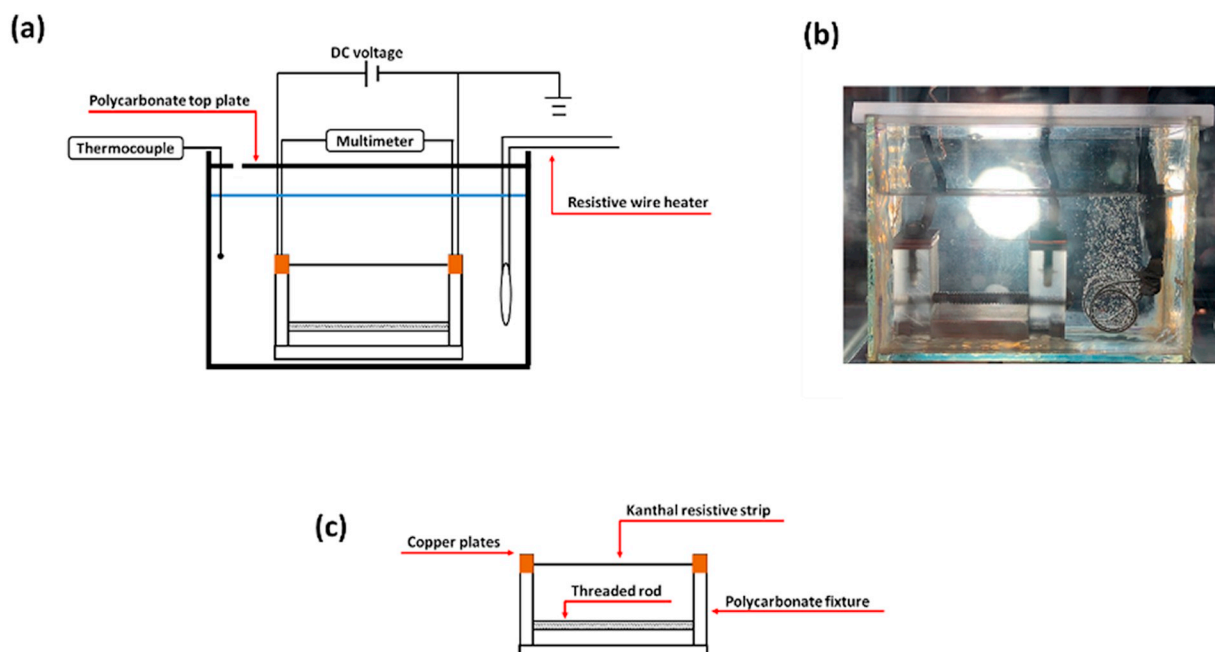


Fig. 1. The experimental setup. (a) Schematic, and (b) the image. (c) Detailed sketch of the specially designed fixture with clamped flat Kanthal resistive strip.

Download English Version:

<https://daneshyari.com/en/article/11029981>

Download Persian Version:

<https://daneshyari.com/article/11029981>

[Daneshyari.com](https://daneshyari.com)